A COMPUTATIONALLY EFFICIENT MODEL FOR SIMULATING AEROSOL INTERACTIONS AND CHEMISTRY (MOSAIC)

Rahul A. Zaveri,[1] Richard C. Easter,[1] Jerome D. Fast,[1] and Leonard K. Peters[2]
[1]Pacific Northwest National Laboratory, Richland, WA
[2]Global Laboratory Operations, Battelle, Richland, WA

Introduction

Atmospheric aerosols are ubiquitous suspended particulate matter that can range from a few nanometers up to a few microns in size. In large urban areas and mega-cities, anthropogenic aerosols are implicated in many human health related problems [Gauderman et al., 2000; Osornio-Vargas et al., 2003; Pope et al., 2004]. On regional and global scales, these as well as other naturally occurring aerosols directly influence the Earth's radiation balance by scattering and absorption of radiation, and indirectly through their impact on cloud microphysical properties and amount [Intergovernmental Panel on Climate Change, 2001]. The role of aerosols in climate forcing is, therefore, a critical factor in climate change assessment, as well as an essential element in advancing the state of the art in climate modeling. As a result, there is an urgent need for developing accurate yet computationally efficient models of aerosol chemistry and microphysics for use in air quality and climate models. This paper describes a new Model for Simulating Aerosol Interactions and Chemistry (MOSAIC), with a special focus on addressing the long-standing issues in solving the dynamic partitioning of semi-volatile inorganic gases (HNO_3, HCl, and NH_3) to size-distributed atmospheric aerosol particles.

MOSAIC Framework

MOSAIC is made highly modular to allow easy coupling between various chemical and microphysical processes. It treats all the major aerosol species important at urban, regional, and global scales, which include sulfate (SULF = SO_4^{2-} + HSO_4^-), methanesulfonate (CH_3SO_3), nitrate (NO_3), chloride (Cl), carbonate (CO_3), ammonium (NH_4), sodium (Na), calcium (Ca), black carbon (BC), primary organic mass (OC), and liquid water (W). Other unspecified inorganic species such as silica (SiO_2), other inert minerals, and trace metals are lumped together as "other inorganic mass" (OIN). The gas-phase species that are allowed to partition to the particle-phase include H_2SO_4, HNO_3, HCl, NH_3, and MSA (methanesulfonic acid). Work is currently underway to include secondary organic aerosols (SOA).

The urban to global scale trace gas photochemistry in MOSAIC is presently modeled with the "lumped-structure" photochemical mechanism CBM-Z [Zaveri and Peters, 1999], which affords a reasonable tradeoff between accuracy and computational efficiency. A condensed dimethylsulfide (DMS) photooxidation

mechanism [Zaveri, 1997] has also been added to simulate the temperature dependent formation of SO_2, H_2SO_4, and MSA in the marine environment. The augmented CBM-Z scheme consists of 67 prognostic species and 164 reactions.

In the present study, MOSAIC is implemented in the sectional framework where the aerosol size distribution is divided into discrete size bins. Each bin is assumed to be internally mixed so that all particles within a bin have the same chemical composition, while particles in different bins are externally mixed. The number of bins is flexible and can be specified by the user. Both mass and number are simulated for each bin. Particle growth or shrinkage resulting from the dynamic gas-particle partitioning of trace gases (H_2SO_4, CH_3SO_3H, HNO_3, HCl, NH_3, and eventually secondary organic species) is first calculated in a Lagrangian manner. Transfer of particles between bins is then calculated using the (default) two-moment approach of Simmel and Wurzler [2006] or the moving section approach of Jacobson [1997]. Aerosol coagulation is calculated using the algorithm of Jacobson et al. [1994] with a Brownian coagulation kernel. H_2SO_4-H_2O homogeneous nucleation is modeled with Wexler et al. [1994] parameterization.

The thermodynamics module in MOSAIC is specially designed for use in dynamic gas-particle partitioning aerosol models, and is both accurate and computational efficient. It consists of the recently developed Multicomponent Taylor Expansion Method (MTEM) to calculate the activity coefficients in aqueous atmospheric aerosols [Zaveri et al., 2005a] and a computationally efficient Multicomponent Equilibrium Solver for Aerosols (MESA) to compute the intra-particle solid-liquid phase equilibrium [Zaveri et al., 2005b].

Gas-particle partitioning of semi-volatile species is a highly dynamic and competitive process, and plays an important role in the continuous evolution of atmospheric aerosols and the associated physical and chemical properties relevant for the climate forcing and air quality issues. The coupled ordinary differential equations (ODE) for dynamic gas-particle mass transfer are extremely stiff, and the available numerical techniques are either inaccurate, very expensive, or produce oscillatory solutions [e.g., Capaldo et al., 2000; Pilinis et al., 2000; Koo et al., 2003; Jacobson, 2005]. These limitations are overcome in MOSAIC with a new dynamic gas-particle partitioning algorithm called ASTEM, which is briefly described below.

Dynamic Gas-Particle Mass Transfer Algorithm: ASTEM

ASTEM stands for Adaptive Step Time-split Euler Method. It is specially designed to take advantage of several prominent characteristics of the atmospheric gas-particle partitioning problem to systematically reduce the stiffness while still maintaining the overall fidelity of the numerical solution. The first step in reducing the stiffness involves separating the non-volatile gases from semi-volatile ones in the numerical solver. Because gases such as H_2SO_4 and MSA are non-volatile, their solution is relatively straightforward and does not

depend on the phase state of the particles in different bins. On the other hand, mass transfer of semi-volatile HNO_3, HCl, and NH_3 is rather complex and depends greatly on the phase-state of the aerosols. Thus, ASTEM consists of two parts which are time-split. In the first part, ASTEM analytically integrates the condensation of non-volatile gases H_2SO_4 and MSA for all the bins over a user-specified time splitting interval, h_{ASTEM}, typically set at 5 min. In the second part, it numerically integrates condensation and/or evaporation of HNO_3, HCl, and NH_3 for all the bins over h_{ASTEM} using adaptive time steps, h. The two parts are described below.

Part 1: Condensation of H_2SO_4 and MSA

Since H_2SO_4 and MSA are non-volatile, it is reasonable to assume their equilibrium surface concentrations to be zero. Furthermore, by assuming that the mass transfer coefficients of H_2SO_4 and MSA for all the bins remain constant over h_{ASTEM}, the condensation of these non-volatile gases reduces to a simple first order process. If H_2SO_4 and MSA condense on particles containing any one or mixture of salts such as $CaCO_3$, $Ca(NO_3)_2$, $CaCl_2$, $NaNO_3$, and NaCl, then the equivalent amounts of CO_2, HCl, and HNO_3 gases are evaporated due to the displacement reactions. However, if any of these salts are not present in the pre-existing aerosol bins, then some NH_3 is allowed to condense so that the aerosols do not artificially become “sulfate rich” before HNO_3, HCl, and additional NH_3 are condensed or evaporated in the next part. Once the new particle-phase sulfate, CH_3SO_3, and NH_4 concentrations are computed, the internal solid-liquid phase equilibrium in each size bin is updated with the thermodynamic module MESA.

Part 2: Condensation/Evaporation of HNO_3, HCl, and NH_3

The gas-particle mass transfer rates of HNO_3, HCl, and NH_3 greatly depend on whether the particles are completely solid, completely liquid, or mixed phase. It is then necessary to explicitly track the aerosol species concentrations in both the solid and liquid phases during each time step taken to integrate HNO_3, HCl, and NH_3. Formulae for computing the gas-particle mass transfer fluxes are described in detail in Zaveri et al. [2008]. The numerical solution for the dynamic mass transfer consists of a combination of semi-implicit and explicit Euler methods for the gas-liquid and gas-solid systems, respectively.

The ASTEM algorithm also includes a new concept of “dynamic pH” and an adaptive time-stepping scheme were developed to further reduce the stiffness in liquid particles, and thereby allow the solver to take long time steps (~100 s) and still produce smooth and accurate solutions over the entire relative humidity range. Dynamic pH is a function of equilibrium constants, mass transfer coefficients, and the gas- and particle-phase concentrations of all the involved species, and is equal to equilibrium pH at steady state. This approach provides for the first time a more accurate calculation of aerosol pH in gas-aerosol systems at non-equilibrium compared to other formulations that are based on

intra-particle thermodynamic equilibrium only. The dynamic pH approach not only eliminates the spurious oscillations typically seen in numerical solutions that are based on equilibrium pH [e.g., Jacobson, 2005], but also significantly speeds up the numerical solution.

Results and Discussion

We first evaluate MOSAIC in the box-model format with a focus on validating the new ASTEM algorithm. We then evaluate MOSAIC within PNNL's 3-D chemical transport model PEGASUS using the 1987 Southern California Air Quality Study (SCAQS) dataset.

Box-Model Results

MOSAIC/ASTEM is evaluated here using 10 idealized test cases which represent different inorganic gas-aerosol systems commonly found in the urban, rural, and marine troposphere [Zaveri et al., 2008]. The time-dependent gas and aerosol concentrations are verified against those computed with a more rigorous but computationally expensive version of the model that uses LSODES (Livermore Solver for Ordinary Differential Equations with general Sparse Jacobian matrix) [Hindmarsh, 1983] instead of ASTEM for directly integrating the gas-particle partitioning equations. These test cases consist of monodisperse (i.e., single-bin) aerosols so that the steady-state MOSAIC results can also be validated against the highly accurate equilibrium model AIM, which serves as another independent benchmark for accuracy [Wexler and Clegg, 2002]. We also compare the steady-state MOSAIC results and the CPU time requirements for these test cases with those obtained with the computationally efficient equilibrium model ISORROPIA [Nenes et al., 1998, 1999].

Figure 1 shows the time evolution of gas and particle concentrations for cases 1-3 at low RH where the given aerosols are completely solid. Figure 2 shows the results for cases 4-7 at high RH where the given aerosols are completely liquid. Figure 3 shows the results for cases 8-10 at moderate RH where the given aerosols contain both the solid and liquid phases. In all cases, MOSAIC/ASTEM predictions (lines) are in excellent agreement with the MOSAIC/LSODES results (filled circles), and the final steady-state solutions matched the AIM equilibrium results (filled squares) almost exactly. On the other hand, the ISORROPIA equilibrium results (filled triangles) show significant deviations from MOSAIC and AIM predictions in solid and mixed-phase test cases. ISORROPIA results were in very good agreement with MOSAIC and AIM for most of liquid cases. However, H^+ ion concentrations predicted by ISORROPIA had large errors compared to MOSAIC and AIM. Finally, despite using long time steps of 100 s at all times, MOSAIC/ASTEM produced smooth and accurate solutions in all the cases.

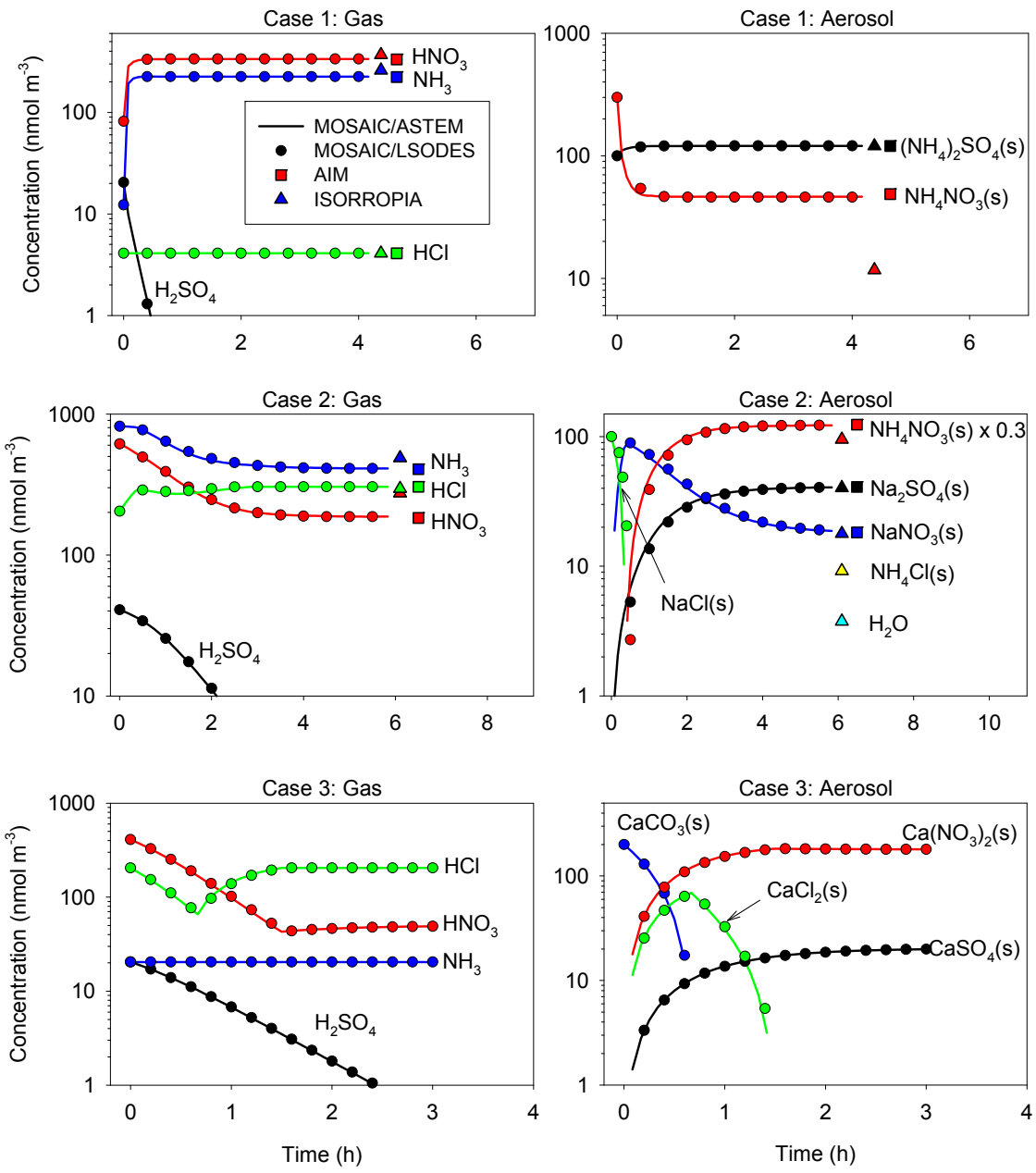

Figure 1. Comparison of the predicted gas and aerosol species from MOSAIC/ASTEM (lines), MOSAIC/LSODES (filled circles), equilibrium ISORROPIA (filled triangles), and equilibrium AIM Model III (filled squares) for completely solid aerosol test cases 1-3. Note that AIM predictions are not included for case 10 which contains calcium.

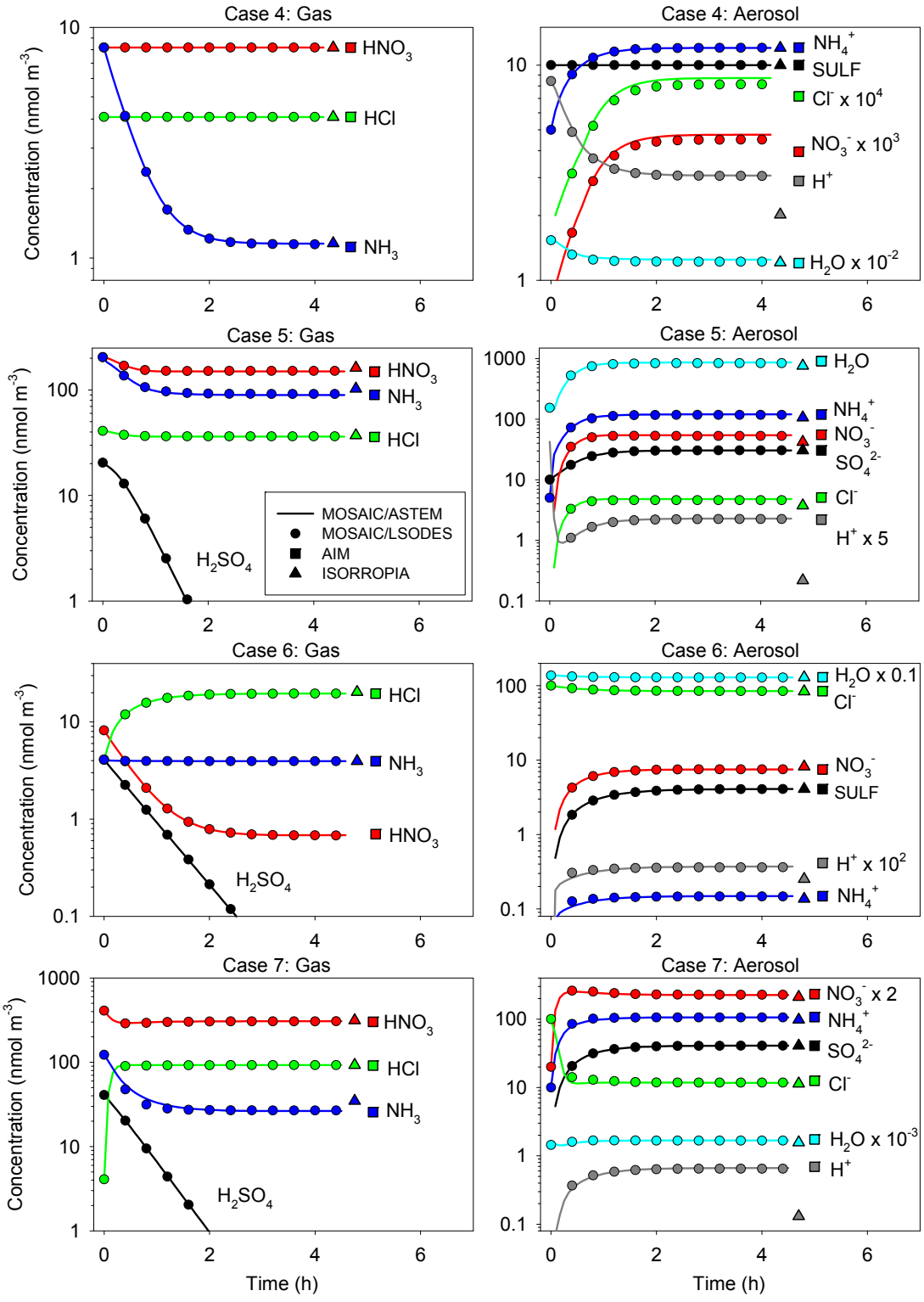

Figure 2. Comparison of the predicted gas and aerosol species from MOSAIC/ASTEM (lines), MOSAIC/LSODES (filled circles), equilibrium ISORROPIA (filled triangles), and equilibrium AIM Model III (filled squares) for completely liquid aerosol test cases 4-7.

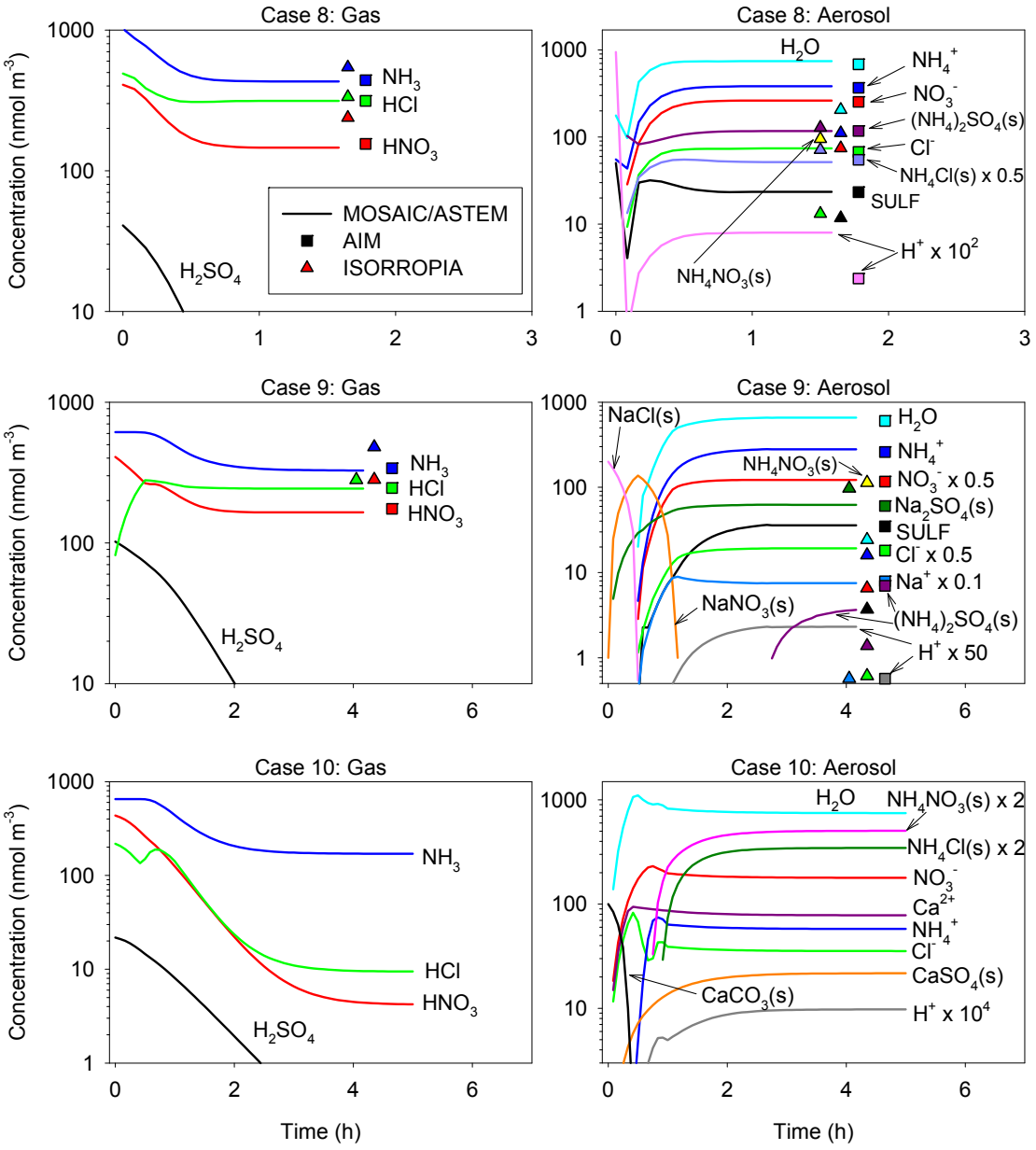

Figure 3. Comparison of the predicted gas and aerosol species from MOSAIC/ASTEM (lines), equilibrium ISORROPIA (filled triangles), and equilibrium AIM Model III (filled squares) for mixed-phase aerosol test cases 8-10. Note that ISORROPIA and AIM predictions are not included for case 10 which contains calcium. LSODES had difficulty converging for the mixed-phase cases, and therefore MOSAIC/LSODES results are not shown in the comparisons.

3-D Model Results

The above box-model tests and analysis verifies and validates the accuracy and robustness of the new thermodynamic and gas-particle partitioning modules in MOSAIC under widely different chemical and RH conditions. we now evaluate MOSAIC within a comprehensive 3-D Eulerian chemical transport model, with the primary goal of estimating its computational efficiency under more realistic ambient conditions and continuously changing meteorological controls. To this end, MOSAIC was implemented in PNNL's Eulerian Gas and Aerosol Scalable Unified System (PEGASUS) [Fast et al., 2002] and applied to simulate trace gas and aerosol evolution in the Los Angeles basin between 08 UTC 26 August and 06 UTC 29 August during the 1987 Southern California Air Quality Study (SCAQS). The model domain was resolved with 78 x 28 x 31 grid points in the X, Y, and Z dimensions, respectively, which gives a total of 67,704 grid cells. The horizontal grid resolution was 5 X 5 km^2 while the vertical grid was non-uniformly spaced. Both the transport-chemistry time splitting interval and ASTEM time splitting interval were set at 300 s, and the maximum allowable internal time step in ASTEM was restricted to 100 s.

Pollutants emitted in downtown Los Angeles were transported primarily from west to east during each afternoon for 3-day period simulated here. Because of photochemical production of secondary aerosol species, the highest particulate mass concentrations were usually measured at the downwind Claremont and Riverside sites located ~50 km and ~75 km east of downtown Los Angeles, respectively. Model performance at the central Los Angeles and Claremont sites only are therefore chosen in the present evaluation for brevity. The predicted diurnal and spatial variations in ozone and particulate matter (not shown) were consistent with the observations, with the peak values east of Los Angeles in the late afternoon. Figure 4 shows comparisons of the predicted (line) and observed (filled circles) diurnal variations in several key gas and particulate (PM2.5) species concentrations at the central Los Angeles and Claremont sites. The predicted values are averages of the values in the grid cell closest to the site and the eight horizontally-adjacent grid cells. The gray shading represents the range of the lowest and the highest values predicted in these nine grid cells. The predicted (average) and observed O_3 diurnal profiles are in excellent agreement, and the small differences between the minimum and maximum values in the nine grid cells indicate relatively weak horizontal gradients in O_3 concentrations at the two sites. On the other hand, relatively larger differences in the predicted minimum and maximum concentrations are seen for various aerosol species, indicating sharp gradients for aerosols at the two sites. As a result the predicted aerosol concentrations are sensitive to small errors in winds and the associated meteorological transport at these and other observation sites. Nevertheless, the predicted average concentrations for the various gas and particulate species agree quite well with the observations at the central Los Angeles and Claremont sites. The model tends to overpredict the concentrations of NH_3 and HNO_3 in the gas phase as well as particulate NH_4 and NO_3 at Claremont, although the

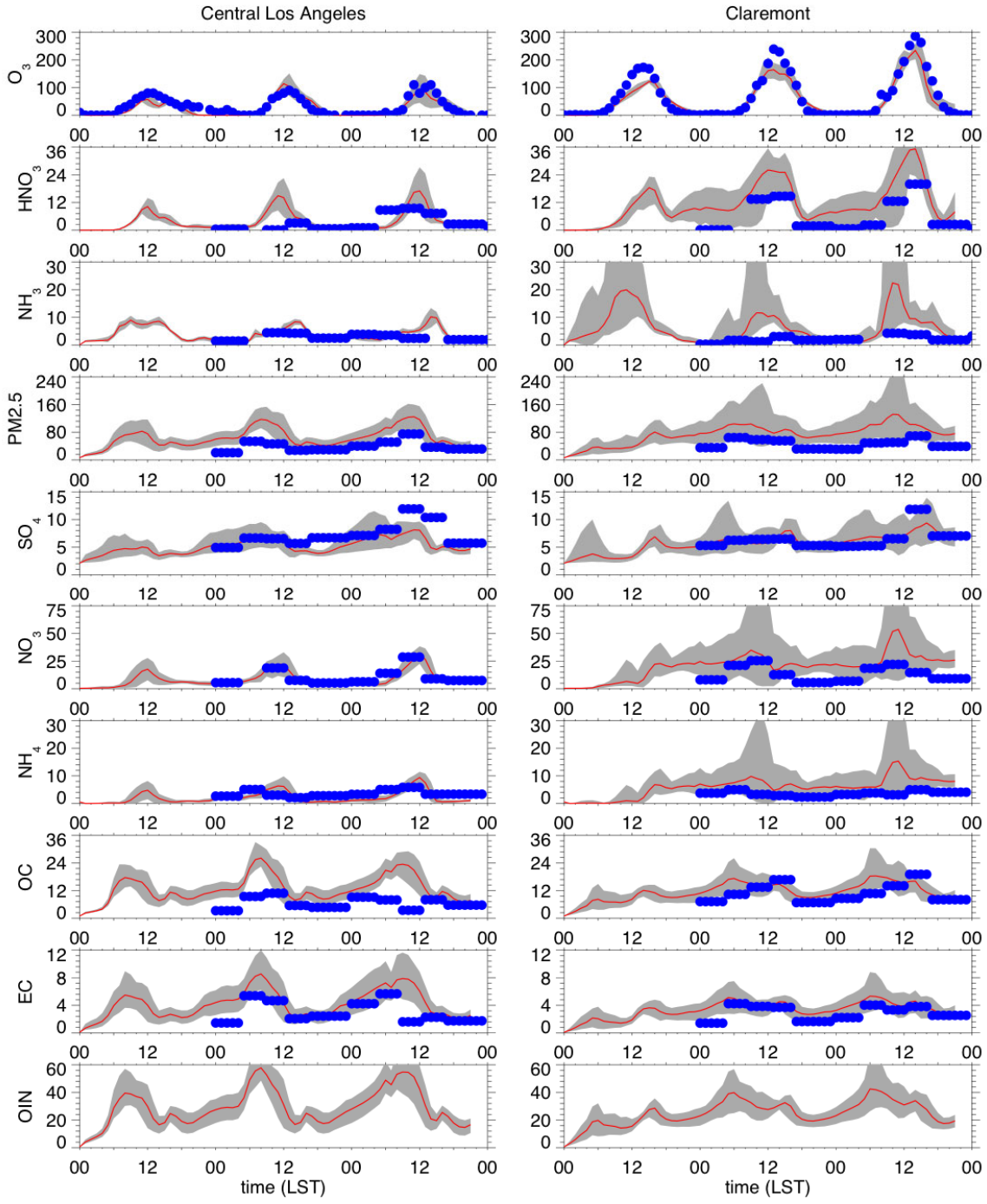

Figure 8. Comparison of the predicted (line) and observed (filled circles) diurnal variations in several key gas (ppbv) and aerosol ($\mu g\ m^{-3}$) species concentrations at the central Los Angeles and Claremont sites. The lines represent average of the values in the grid cell closest to the site and the eight horizontally-adjacent grid cells. The gray shading represents the range of the lowest and the highest values predicted in these nine grid cells.

minimum of the nine grid cells compared well with the observations. This suggests that the discrepancies between model predictions and observations at Claremont are likely due errors/uncertainties in transport and mixing and/or in the emission inventory for NO_x and NH_3. The predicted PM2.5 mass was somewhat higher than observed at Los Angeles as a result of high organic carbon and other inorganic mass, while predicted PM2.5 was higher than observed at Claremont as a result of nitrate and other inorganic mass. Unfortunately, there were no measurements of other inorganic mass to directly evaluate the model for this species. The reason predicted organic carbon was similar to the measurements even though MOSAIC does not presently treat SOA is that emissions of organic carbon were increased from the original estimates as in Zhang et al. [2004].

Computational Efficiency

The CPU timing tests for the box-model tests showed that MOSAIC/ASTEM is two orders of magnitude faster than MOSAIC/LSODES. MOSAIC's efficiency was also determined by comparing its CPU speed with that of ISORROPIA, which is considered to be one of the fastest equilibrium models currently available [Ansari and Pandis, 1999]. Since MOSAIC is a fully dynamic model, we compare its average CPU time requirement per size bin per 5 min integration interval (typical 3-D model time step) to the CPU time requirement per single, bulk equilibrium calculation with ISORROPIA. The codes were tested with three different compilers (Portland Group Fortran 77/90, PathScale Fortran 77/90, and Intel Fortran 77/90) on two different Linux workstation platforms (3.0 GHz Intel Xeon and 3.0 GHz Intel EM64T processors). The CPU time requirements for MOSAIC and ISORROPIA were found to be similar for most of the cases tested in this study. However, for some test cases, MOSAIC was found to be up to 20 times faster ISORROPIA. At the same time, MOSAIC was also found to be much more accurate than ISORROPIA under these conditions as discussed earlier.

For the 3-D model test, the 3-day Los Angeles Basin simulation took ~1 CPU day. The average CPU time per grid cell per hour was ~20 ms of which 12 ms (60% of the total CPU time) was taken up by the dynamic gas-particle partitioning, thermodynamic equilibrium, and sectional growth calculations in MOSAIC. This corresponds to an average CPU time of 125 μs per bin per 5 min, which is comparable to the range of CPU times seen for the box-model tests cases.

While more comprehensive comparisons of accuracy and efficiency of MOSAIC with other dynamic models are warranted in the future, the present study demonstrates that MOSAIC is extremely efficient without sacrificing accuracy, and is therefore highly attractive for use in large scale, 3-D air quality and aerosol models.

Summary

We have described the various chemical, thermodynamic, and microphysical processes currently represented in the new aerosol model MOSAIC (Model for Simulating Aerosol Interactions and Chemistry), with a special focus on addressing the long-standing problems in dynamic gas-particle partitioning of semi-volatile inorganic species. The coupled ordinary differential equations describing the dynamic gas-particle mass transfer process are stiff and have proved to be extremely difficult to solve – the numerical techniques available in the literature are either computationally too expensive or produce oscillatory and/or inaccurate steady-state results. These problems were overcome in MOSAIC with a new dynamic gas-particle partitioning solver ASTEM (Adaptive Step Time-split Euler Method). The ASTEM algorithm reduces the stiffness in the ODEs by first analytically solving the condensation of all the non-volatile gases (H_2SO_4 and CH_3SO_3H) over a time-splitting interval, which is typically set at ~300 s. This is then followed by a numerical solution for the dynamic mass transfer of semi-volatile gases (HNO_3, HCl, and NH_3) over the same time interval with a combination of semi-implicit and explicit Euler methods for the gas-liquid and gas-solid systems, respectively. A new concept of "dynamic pH" and an adaptive time-stepping scheme were developed to further reduce the stiffness in liquid particles, and thereby allow the solver to take long time steps (~100 s) and still produce smooth and accurate solutions over the entire relative humidity range.

MOSAIC was evaluated for several test cases representing different gas-aerosol systems commonly found in the troposphere. Performance of the new ASTEM solver was verified against a benchmark version of MOSAIC that uses the stiff ODE solver LSODES to rigorously integrate the dynamic mass transfer of all the species simultaneously without the numerical approximations used in ASTEM. The time-varying predictions with MOSAIC/ASTEM and MOSAIC/LSODES were found to be in excellent agreement for all the cases (monodisperse and polydisperse aerosols) tested under low and high RH conditions, thus validating the ASTEM algorithm. Furthermore, the final (steady-state) MOSAIC results were in excellent agreement with those obtained with the benchmark equilibrium model AIM for the monodisperse aerosol test cases at low, moderate, and high RH. On the other hand, aerosol composition, concentration, water content, and pH predicted by the computationally efficient equilibrium model ISORROPIA were also in very good agreement with AIM and MOSAIC for most of the high RH test cases, but relatively larger errors were seen under low and moderate RH conditions. Furthermore, the CPU times required for dynamic solutions by MOSAIC per size bin per 5 min integration interval (typical 3-D model time step) were similar to the CPU times required for single, bulk equilibrium solutions by ISORROPIA, although in some instances MOSAIC took ~20 times less CPU time than ISORROPIA. For the polydisperse aerosol test cases, MOSAIC/ASTEM was found to be 100-300 times faster than MOSAIC/LSODES.

An eight-bin version of MOSAIC was then applied and evaluated within Pacific Northwest National Laboratory's offline 3-D chemical transport model PEGASUS for southern California area using the historic 1987 SCAQS dataset. The primary goal of this exercise was to estimate MOSAIC's computational efficiency under more realistic conditions. Simulated diurnal gas and aerosol variations at the central Los Angeles and downwind Claremont sites compared well with the observations. The total CPU time per grid cell per hour averaged over the entire simulation was 20 ms (on a 3.0 GHz Intel Xeon processor), ~60% of which was used up by aerosol calculations in MOSAIC. These results show that MOSAIC is extremely efficient without compromising accuracy, and is therefore highly attractive for use in 3-D air quality and large scale aerosol models.

Acknowledgements

The authors thank A. Nenes of Georgia Tech, Atlanta, for providing a copy of the ISORROPIA code and assisting in comparing its performance with MOSAIC. Funding for this research was provided by the U.S. Department of Energy (DOE) under the auspices of the Atmospheric Science Program of the Office of Biological and Environmental Research, the NASA Earth Science Enterprise under grant NAGW 3367, and Pacific Northwest National Laboratory (PNNL) Laboratory Directed Research and Development (LDRD) program. Pacific Northwest National Laboratory is operated for the U.S. Department of Energy by Battelle Memorial Institute under contract DE-AC06-76RLO 1830.

References

1. Capaldo, K. P., C. Pilinis, and S. N. Pandis (2000), A computationally efficient hybrid approach for dynamic gas/aerosol transfer in air quality models, *Atmos. Environ. 34*, 3617–3627.
2. Fast, J. D., R. A. Zaveri, X. Bian, E. G. Chapman, and R. C. Easter (2002), Effect of regional-scale transport on oxidants in the vicinity of Philadelphia during the 1999 NE-OPS field campaign, *J. Geophys. Res.*, *107*(D16), 4307, doi:10.1029/2001JD000980.
3. Gauderman W. J., R. McConnell, F. Gilliland, S. London, D. Thomas, E. Avol, H. Vora, K. Berhane, E. B. Rappaport, F. Lurmann, H. G. Margolis, and J. Peters (2000), Association between air pollution and lung function growth in southern California children, *Am. J. Respir. Crit. Care Med.*, *162*, 1383-1390.
4. Hindmarsh, A. C. (1983), ODEPACK, a systematized collection of ODE solvers. In *Scientific Computing*, edited by R. S. Stepleman et al. North-Holland, Amsterdam, pp. 55-64.
5. Intergovernmental Panel on Climate Change (2001), *Climate Change 2001: The Scientific Basis*, Cambridge Univ. Press, New York. (Available at http://www.grida.no/climate/ipcc_tar/)

6. Jacobson, M.Z. (1997), Development and application of a new air pollution modeling system – II. Aerosol module structure and design, *Atmos. Environ.*, *31*, 131-144.
7. Jacobson, M. Z., A solution to the problem of nonequilibrium acid/base gas-particle transfer at long time step, *Aerosol Science and Technology*, *39*, 92–103, 2005.
8. Jacobson, M. Z., R. P. Turco, E. J. Jensen, and O. B. Toon (1994), Modeling coagulation among particles of different composition and size, *Atmos. Environ.*, *28*, 1327-1338.
9. Koo, B., T. M. Gaydos, and S. N. Pandis (2003), Evaluation of the equilibrium, dynamic, and hybrid aerosol modeling approaches, *Aerosol. Sci. Technol.*, *37*, 53–64.
10. Nenes, A., S. N. Pandis, and C. Pilinis (1998), ISORROPIA: A new thermodynamic equilibrium model for multiphase multicomponent inorganic aerosols, *Aquatic Geochem.*, *4*, 123–152.
11. Nenes, A., C. Pilinis, and S. N. Pandis (1999), Continued development and testing of a new thermodynamic aerosol module for urban and regional air quality models, *Atmos. Environ.*, *33*, 1553–1560.
12. Osornio-Vargas, A. R., J. C. Bonner, E. Alfaro-Moreno, L. Martinez, C. Garcia-Cuellar, S. P. Rosales, J. Miranda, and I. Rosas (2003), Proinflammatory and cytotoxic effects of Mexico City air pollution particulate matter *in vitro* are dependent on particle size and composition, *Environ. Health Perspectives*, *111*, 1289–1293.
13. Pilinis C., K. P. Capaldo, A. Nenes, and S. N. Pandis (2000), MADM – A New Multicomponent Aerosol Dynamics Model, *Aerosol Sci. Technol., 32*, 482–502.
14. Pope C. A., R. T. Burnett, G. D. Thurston, M. J. M. Thun, E. Calle, D. Krewski, and J. J. Godleski (2004), Cardiovascular mortality and long term exposure to particulate air pollution, *Circulation*, *109*, 71-77.
15. Wexler, A. S., F. W. Lurmann, and J. H. Seinfeld (1994), Modelling urban and regional aerosols – I. Model development, *Atmos. Environ.*, *28*, 531-546.
16. Wexler A. S., and S. L. Clegg (2002), Atmospheric aerosol models for systems including the ions H^+, NH_4^+, Na^+, SO_4^{2-}, NO_3^-, Cl^-, Br^-, and H_2O, *J. Geophys. Res.*, *107*(D14), 4207, doi:10.1029/2001JD000451.
17. Zaveri, R. A. (1997), Development and evaluation of a comprehensive tropospheric chemistry model for regional and global applications, Ph.D. thesis, Va. Polytech. Inst. and State Univ., Blacksburg, Va.
18. Zaveri, R. A., and L. K. Peters (1999), A new lumped structure photochemical mechanism for large-scale applications, *J. Geophys. Res., 104*, 30387-30415.
19. Zaveri, R. A., R. C. Easter, and A. S. Wexler (2005a), A new method for multicomponent activity coefficients of electrolytes in aqueous atmospheric aerosols, *J. Geophys. Res.*, *110*, D02201, doi:10.1029/2004JD004681.

20. Zaveri, R. A., R. C. Easter, and L. K. Peters (2005b), A computationally efficient Multicomponent Equilibrium Solver for Aerosols (MESA), *J. Geophys. Res. 110*, D24203, doi:10.1029/2004JD005618.
21. Zaveri, R. A., R. C. Easter, J. D. Fast, and L. K. Peters (2008), Model for Simulating Aerosol Interactions and Chemistry (MOSAIC), *J. Geophys. Res.,* 113, D13204, doi:10.1029/2007JD008782.
22. Zhang, Y., B. Pun, K. Vijayaraghavan, S.-Y. Wu, C. Seigneur, S. N. Pandis, M. Z. Jacobson, A. Nenes, and J. H. Seinfeld (2004), Development and application of the Model of Aerosol Dynamics, Reaction, Ionization, and Dissolution (MADRID), *J. Geophys. Res.*, *109*, D01202, doi:10.1029/2003JD003501.